Journal of Hydrology 547 (2017) 332–344

Contents lists available at ScienceDirect

Journal of Hydrology

journal homepage: www.elsevier.com/locate/jhydrol

Research papers

The impact of green roof ageing on substrate characteristics and hydrological performance

Simon De-Ville [a,*], Manoj Menon [b], Xiaodong Jia [c], George Reed [a], Virginia Stovin [a]

[a] Department of Civil & Structural Engineering, University of Sheffield, Sir Frederick Mappin Building, Mappin Street, Sheffield S1 3JD, UK
[b] Department of Geography, University of Sheffield, Sheffield S10 2TN, UK
[c] School of Chemical and Process Engineering, University of Leeds, Leeds LS2 9JT, UK

ARTICLE INFO

Article history:
Received 23 September 2016
Received in revised form 13 January 2017
Accepted 6 February 2017
Available online 9 February 2017
This manuscript was handled by Tim R. McVicar, Editor-in-Chief, with the assistance of Giorgio Mannina, Associate Editor

Keywords:
Green roof
Substrate
Physical properties
Hydrological performance
Ageing
X-ray microtomography

ABSTRACT

Green roofs contribute to stormwater management through the retention of rainfall and the detention of runoff. However, there is very limited knowledge concerning the evolution of green roof hydrological performance with system age. This study presents a non-invasive technique which allows for repeatable determination of key substrate characteristics over time, and evaluates the impact of observed substrate changes on hydrological performance.

The physical properties of 12 green roof substrate cores have been evaluated using non-invasive X-ray microtomography (XMT) imaging. The cores comprised three replicates of two contrasting substrate types at two different ages: unused virgin samples; and 5-year-old samples from existing green roof test beds. Whilst significant structural differences (density, pore and particle sizes, tortuosity) between virgin and aged samples of a crushed brick substrate were observed, these differences did not significantly affect hydrological characteristics (maximum water holding capacity and saturated hydraulic conductivity). A contrasting substrate based upon a light expanded clay aggregate experienced increases in the number of fine particles and pores over time, which led to increases in maximum water holding capacity of 7%. In both substrates, the saturated hydraulic conductivity estimated from the XMT images was lower in aged compared with virgin samples. Comparisons between physically-derived and XMT-derived substrate hydrological properties showed that similar values and trends in the data were identified, confirming the suitability of the non-invasive XMT technique for monitoring changes in engineered substrates over time.

The observed effects of ageing on hydrological performance were modelled as two distinct hydrological processes, retention and detention. Retention performance was determined via a moisture-flux model using physically-derived values of virgin and aged maximum water holding capacity. Increased water holding capacity with age increases the potential for retention performance. However, seasonal variations in retention performance greatly exceed those associated with the observed age-related increases in water holding capacity (+72% vs +7% respectively). Detention performance was determined via an unsaturated-flow finite element model, using van Genuchten parameters and XMT-derived values of saturated hydraulic conductivity. Reduced saturated hydraulic conductivity increases detention performance. For a 1-hour 30-year design storm, the peak runoff was found to be 33% lower for the aged brick-based substrate compared with its virgin counterpart.

1. Introduction

A green roof is an example of a Sustainable Drainage System (SuDS) which provides stormwater quantity management benefits through two hydrological processes. The first is retention (the permanent removal of rainfall) and the second is detention (the transient storage of rainfall as it passes through the roof layers). As green roof systems age, their living components – particularly the vegetation, but also the substrate – are subject to a number of processes that have the potential to alter system-wide hydrological performance (Berndtsson, 2010). Some of these processes are well understood. For example, the daily and seasonal changes in evapotranspiration are known to control a green roof's retention performance (Poë et al., 2015). The effects of other key processes, such as root system development, organic matter turnover,

* Corresponding author.
E-mail address: sde-ville1@sheffield.ac.uk (S. De-Ville).

http://dx.doi.org/10.1016/j.jhydrol.2017.02.006
0022-1694/

weathering and substrate consolidation, are less well understood in the context of green roof hydrological performance (Berndtsson, 2010).

1.1. Green roof hydrological performance

Much of the current research into green roof stormwater quantity control (hydrological performance) focusses on short term studies (<1 year), leading to a single overall retention performance value. For example, Harper et al. (2015) stated that over a 9-month period a vegetated green roof was capable of retaining approximately 60% of rainfall. The multi-year study performed by Nawaz et al. (2015) again provided a single mean value of retention performance (66%) for the entire monitoring period. These two recent examples are representative of the wider literature.

Detention performance metrics are less commonly reported due to difficulties in its characterisation. For example, Stovin et al. (2015a) used peak attenuation to characterise and compare detention performance for 9 green roof configurations over a 4-year period. For events with more than 10 mm of rainfall, mean peak attenuation (5-min resolution) was seen to vary from approximately 40 to 70% depending on roof configuration. Reported values from monitoring studies are influenced by rainfall characteristics and antecedent conditions (retention processes). However, the fundamental hydrological detention processes are essentially independent of these factors and dependant only on the green roof's physical configuration (Stovin et al., 2015b). Whilst differences due to configuration and climate have been considered in some depth, there is very little discussion and understanding of the long-term temporal variation that green roof hydrological performance, both retention and detention, may exhibit as a result of system age.

Green roof hydrological performance is a function of the combined effects of a range of interacting physical processes. These processes are in turn influenced by the substrate's physical characteristics, including pore size distribution, particle size distribution, particle shape and texture. It is these physical characteristics that determine key hydrological properties, including density, porosity, hydraulic conductivity and water holding capacity. Green roof detention performance is largely influenced by porosity and hydraulic conductivity, as these properties define the speed with which water can pass through a substrate. Retention performance is related to the pore size distribution which dictates water release characteristics, in turn determining permanent wilting point (PWP) and maximum water holding capacity (MWHC). The maximum potential retention capacity is defined by the difference between PWP and MWHC (often referred to as plant available water, PAW). Whether this capacity is available at the onset of a specific storm event depends on evapotranspiration in the antecedent dry weather period.

1.2. Green roof ageing

In their extensive review of green roof literature, Li and Babcock (2014) identified very few studies addressing the impact that green roof ageing may have upon hydrological performance over time. Whilst this partly reflects the scarcity of long-term hydrological records, the effect that natural climatic variation has on observed hydrological performance is likely to mask any subtle changes in the underlying hydrological characteristics of the system.

Those studies that have considered green roof age and associated substrate property changes have identified very different trends. Mentens et al. (2006), found no correlation between green roof age and yearly runoff quantity for a series of differently-configured German green roofs when analysing less than 5 years of data. Getter et al. (2007) found that substrate organic content and pore volume both doubled over a 5-year period. Getter et al. (2007) hypothesised improvements to retention performance due to an increase in microporosity (<50 μm), but noted these improvements may come at the expense of detention performance due to an increased presence of macropore (>50 μm) channels. Contrastingly, in a study of green roof establishment, Emilsson and Rolf (2005) observed a net loss of organic matter from 3 to 1% over a single year. Bouzouidja et al. (2016) identified similar falls in organic content over a 4 year-period and reported a reduction in the mass of particles smaller than 2 mm in diameter. The impact that organic matter fluctuations can have on green roof hydrological performance is demonstrated by Yio et al. (2013), where a threefold increase in organic content (Coir) was associated with a peak attenuation increase from 15 to >50%.

Beyond the limited range of green roof ageing literature, other SuDS devices provide evidence of ageing effects. Biofilters are prone to sedimentation and clogging as they age, although the media's hydraulic conductivity may be maintained through the presence of plant roots (Virahsawmy et al., 2014). Further literature from the agro/forestry fields provides evidence of the effects that plant-life can have on soil porosity and infiltration rates. Root growth can reduce pore volumes due to local compression and pore filling (Dexter, 1987), thereby reducing hydraulic conductivity. The decay of dead roots leaves channels which may increase pore spaces and act as flow paths, increasing hydraulic conductivity (Schwen et al., 2011). Plant activity can also influence soil aggregation (Lado et al., 2004) and desiccation cracking (Materechera et al., 1992). However, the majority of agro/forestry literature is based on observations of plant species and growing media not typically found on a green roof, which potentially limits its relevance here.

1.3. Evaluating green roof substrate properties

Many current techniques for the evaluation of green roof substrate properties are invasive and destructive. These methods typically involve the collection and aggregation of several samples into an overall sample, which is then used for physical property evaluation (Emilsson and Rolf, 2005; Thuring and Dunnett, 2014). Such methods lead to the destruction of the original pore space distribution, altering porosity and hydraulic conductivity characteristics. Alternatively, in an effort to maintain the particle and pore size distributions, cores of the substrate can be taken and set in resin. This preserves the internal structure of the core, which can then be cut to examine the internal structure. Whilst this technique does preserve the in-situ characteristics of the green roof substrate, it is only capable of providing 2D perspectives of the core as opposed to the full 3D volume (Young et al., 2001).

X-ray microtomography (XMT) is a non-destructive 3D computed tomography (CT) imaging approach, which is widely used for the visualisation and quantification of an object's internal structure. Improvements in spatial resolution and image reconstruction times since the turn of the century have allowed XMT to become a commonly accepted tool for material analysis (Maire and Withers, 2014). Images are obtained by passing X-rays from a suitable source through the object to be imaged and onto a CCD detector. Typical achievable image resolutions range from <1 μm to 150 μm depending upon object size. The resulting high resolution images can be analysed to show the 3D spatial arrangement of the solid particles and pore spaces in a soil matrix.

XMT is an established technique within the soil sciences field, where the main application has been for the characterisation of physical soil properties (Menon et al., 2015). Several studies have successfully utilised XMT to observe plant roots and their interactions with soils, earthworm burrows, soil insects, and other soil microorganisms (Taina et al., 2008). However, there has been

limited use of XMT to image engineered soils similar to those used as green roof substrates. The non-invasive nature of XMT allows for considerably greater preservation of the delicate internal structure of a green roof substrate than is possible with destructive or reconstructive testing techniques. In turn, this enables the reliable characterisation of in-situ substrate properties and further 3D analyses. Previous studies on conventional soils have confirmed that the XMT technique provides comparable or improved results over thin section analysis, vacuum analysis and mercury porosimetry (Taina et al., 2008).

Menon et al. (2011, 2015) have demonstrated the implementation of the Lattice Boltzmann Method (LBM) for evaluating fluid flow through soil matrices, by utilising 3D XMT images. These fluid flow simulations permit the estimation of permeability and saturated hydraulic conductivity (K_{sat}). The LBM method is a preferable alternative to other conventional Computational Fluid Dynamics (CFD) approaches due to its ability to use large datasets with complex irregular geometries and its speed (particularly when also considering the meshing requirement of conventional CFD approaches) (Menon et al., 2011). The LBM method is uniquely suited to the saturated hydraulic conductivity modelling of complex soil/substrate matrices obtained from 3D XMT images.

1.4. Green roof modelling

Stovin et al. (2015b) provides a short review of the various approaches to green roof hydrological modelling presented in the literature. Numerous statistical regression models have been developed to predict hydrological performance for specific roof configurations in specific climates (Carson et al., 2013; Fassman-Beck et al., 2013). However, the use of physically-based models provides a more generic modelling option (Stovin et al., 2012). It has been identified that proper representation of evapotranspiration processes is critical for the continuous simulation of green roof retention performance (Jarrett and Berghage, 2008; Stovin et al., 2013). This representation is commonly achieved through a substrate moisture flux approach, which has been shown to reliably predict retention performance (Stovin et al., 2013; Locatelli et al., 2014).

Combining retention and detention processes allows the prediction of temporal runoff profiles. Techniques used to model detention include: finite element solutions of the unsaturated flow equations (Hilten et al., 2008; Palla et al., 2011); a unit hydrograph-based approach (Villarreal and Bengtsson, 2005); and a simple reservoir routing technique (Jarrett and Berghage, 2008; Kasmin et al., 2010). Each method has been shown to demonstrate acceptable levels of accuracy for stormwater modelling requirements (Villarreal and Bengtsson, 2005; Hilten et al., 2008; Jarrett and Berghage, 2008; Kasmin et al., 2010; Palla et al., 2011). Whilst the unit hydrograph and the reservoir routing approaches rely on previously-monitored data for calibration, the physically-based finite element models potentially provide a generic approach capable of estimating detention processes in unmonitored systems. However, these models are reliant on a large number of substrate properties, several of which are difficult to obtain using traditional laboratory techniques (e.g. water release curve, pore size distribution). The XMT technique may provide an easier method for the assessment of these critical substrate properties.

1.5. Study objectives

This study aims to test the null hypothesis that substrate physical properties, and therefore hydrological performance, are constant with age. This is achieved via the following objectives:

- *Objective 1:* Characterise the physical properties of virgin and aged green roof substrates via physical (destructive) tests, non-invasive XMT techniques and numerical modelling. This is addressed in Sections 2 and 3;
- *Objective 2:* Evaluate the differences in physical properties between two distinct green roof substrate types to identify any differences in their response to ageing processes. This is addressed in Sections 3 and 4;
- *Objective 3:* Assess the impact that any variation in substrate properties has on hydrological performance using appropriate modelling tools. This is addressed in Sections 3 and 4;
- *Objective 4:* Determine the usefulness of non-invasive X-ray microtomography (XMT) in evaluating the physical properties of green roof substrates. This is addressed in Section 4.

2. Methods

2.1. Substrate types for investigation

Previous green roof studies by Berretta et al. (2014) and Poë et al. (2015) both considered three types of green roof substrate; two brick-based varieties and an expanded clay variety, which are all Forschungsgesellschaft Landschaftsentwicklung Landschaftsbau, (FLL, 2008) compliant. The FLL is a German guideline for the planning, construction and maintenance of green roofing and is widely cited internationally. Stovin et al. (2015a) identified that there were minimal differences in the hydrological performance of the two brick-based substrates. Therefore, the present study evaluates a single crushed brick-based substrate and an expanded clay-based substrate. The crushed brick-based substrate (BBS) is typical of many extensive green roof substrate mixes. The mineral component consists of crushed terracotta brick (55%) and pumice (30%). The organic components are coir (10%) and bark (5%). The second substrate is based on a Light Expanded Clay Aggregate (LECA), which is the sole mineral component (80%). The organic component is compost (10%) and the remainder is loam (10%). This LECA substrate is quite different in physical appearance (Fig. 1) and characteristics compared to BBS.

2.2. Extraction and preparation of substrate cores

Three aged and three virgin cores were obtained for each substrate type. The virgin cores (BBS_V and $LECA_V$) were formed from surplus substrate material used to construct two active green roof test beds. The aged cores (approximately 5 years of age, BBS_A and $LECA_A$) were taken from two active green roof test beds, which included an additional *Sedum* spp. vegetation layer not present in the virgin cores. The aged BBS cores were taken from the Mappin Test Bed (Stovin et al., 2012, provides a full description of this facility) and the aged LECA cores were taken from the Hadfield Test

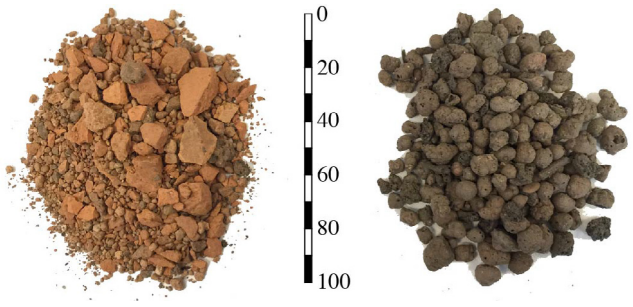

Fig. 1. Left: Crushed brick based substrate (BBS). Right: Light expanded clay aggregate based substrate (LECA). Scale is in mm.

Beds (Berretta et al., 2014, provides a full description of this facility). Cores were driven vertically into the green roof substrates and then carefully removed via excavation of the local area. Above ground plant material remained in place but was not studied or imaged as part of the XMT programme; the roots were maintained and are subsequently treated as particles within the substrate matrix. The core holders were 68 mm in height with an internal diameter of 46 mm, these sizes were dictated by the loading gauge of the XMT machines available. The core holders were constructed from *Poly* (*methyl methacrylate*) (PMMA, commercially known as Perspex). A non-metallic material is required for the XMT imaging process to prevent poor image quality.

2.3. Physical testing of substrates

To maintain the substrate cores' 'in-situ' status for as long as possible, some physical characterisations were not undertaken. However, each of the substrate cores was characterised in line with the FLL (2008) guidance for determining apparent density and maximum water holding capacity using 3 replicates. The solid base of the core holders prevented hydraulic conductivity measurements. On completion of the XMT imaging, samples were destructively tested to determine particle size distributions using a sieve analysis. Cores were not then reconstructed for further testing. Where experimental technique prohibited the determination of certain substrate properties, values previously reported in Poë et al. (2015) and Stovin et al. (2015a) were used (see Table 1).

2.4. XMT image capture and processing

The substrate cores were imaged using a *General Electric v|tome|x M* CT scanner at the University of Nottingham's Hounsfield Facility. Each core was scanned at a resolution of 30 μm and took approximately 30 min to complete, with each scan producing 15 GB of image data.

All sample images were processed following the same image processing protocol (full details of this are available as Supplementary material) using ImageJ and Avizo software (Schneider et al., 2012; FEI, 2015). The following physical substrate properties were identified through image filtering, segmentation and separation: porosity; pore size distribution; particle size distribution and tortuosity. The Lattice Boltzmann method was used to estimate sample saturated hydraulic conductivity from the 3D substrate matrices, as per Menon et al. (2011).

2.5. Green roof hydrological modelling

2.5.1. Retention performance

Retention processes within the substrate were modelled using a conceptual hydrological flux model as presented in Stovin et al. (2013). Runoff was predicted from moisture fluxes within the substrate due to precipitation and evapotranspiration. Runoff volumes were calculated from the following relationships:

$$R_t = \begin{cases} 0, & S_{t-1} + P_t - ET_t \leqslant S_{max} \\ P_t - (S_{max} - S_{t-1}) - ET_t, & S_{t-1} + P_t - ET_t > S_{max} \end{cases} \quad (1)$$

where R is runoff, S is the storage level, P is precipitation, ET is evapotranspiration and S_{max} is the maximum substrate retention capacity (equal to PAW), all in mm; t is the discretised time-step. ET is calculated as a function of Potential Evapotranspiration (PET) by use of a Soil Moisture Extraction Function (SMEF):

$$ET_t = PET_t \times \frac{S_{t-1}}{S_{max}} \quad (2)$$

The retention performance was then calculated by subtracting the total runoff from the total precipitation and dividing by total precipitation.

The retention performance was determined for four design storm scenarios. Two values of S_{max} were assessed; corresponding to an 80 mm depth of virgin and aged substrate. Additionally, two values of PET were assessed; corresponding to typical spring and summer conditions for Sheffield, UK, where PET was 1.8 and 4.5 mm/day respectively (Poë et al., 2015). All runoff volumes were in response to a 1-hour duration 1-in-30-year design rainfall event for Sheffield, UK, and a variable 1–28 day antecedent dry weather period (ADWP). On day zero, S was set equal to S_{max} to simulate field capacity conditions.

Whilst the consideration of a roof's response to an extreme design storm is relevant to flood protection, urban drainage design strategies are also informed by an understanding of a system's response to routine events. Stovin et al. (2013) applied a representative 30-year hourly rainfall time-series for four different UK locations obtained using the UK climate projections weather generator (UKCP09, http://ukclimateprojections.defra.gov.uk/). Long-term retention performance was evaluated for the virgin and aged S_{max} values in response to the 30-year time-series for Sheffield, UK. PET for these long-term simulations was determined from corresponding climate data and the Thornthwaite formula (Wilson, 1990).

2.5.2. Detention performance

Detention performance was determined in isolation from the effects of retention using a Finite Element (FE) model developed and validated by Bayton (2013). The FE model uses a numerical solution of Darcy's Law and the Moisture-Mass Conservation Law to predict runoff volumes for an unsaturated media in response to an input rainfall. An 80 mm substrate depth was modelled with a vertical spatial discretisation of 1 mm using a 0.6 s time-step. The initial model moisture content was set equal to the physically-derived field capacity. The upper substrate surface was subject to a flux, corresponding to a relevant rainfall profile. Two rainfall inputs were used, a 1-hour duration 1-in-30-year design rainfall and a monitored rainfall event. The lower surface was set as a free draining boundary.

The FE model requires the parameters of a van Genuchten water release curve model (van Genuchten, 1980) and a value of K_{sat}. The van Genuchten parameters were determined via the RETC software (van Genuchten et al., 1991) using pressure plate extraction data for comparable brick-based substrates presented by Berretta et al. (2014). The runoff responses for two values of K_{sat} were assessed. These correspond to the XMT-derived mean virgin K_{sat} and mean aged K_{sat} for the BBS substrate. The lack of data for LECA limits detention performance predictions to the BBS substrate only.

Table 1
Substrate physical properties explored in this study and methods of characterisation.

Property	Substrate physical property source		
	Literature	Physical testing	XMT image analysis
Porosity	✓	✓	✓
Particle Size Distribution	✓	✓	✓
Pore Size Distribution	–	–	✓
Dry Density	✓	✓	–
Density at Field Capacity	✓	✓	–
Max. Water Holding Capacity	✓	✓	–
Saturated Hydraulic Conductivity	✓	–	✓
Tortuosity	–	–	✓

3. Results

3.1. Physically-derived substrate properties

Table 2 lists all physically-derived parameters for the two substrate types and ages. Both substrate types show a statistically significant increase in the fraction of finer particles for aged samples (Fig. 2). For BBS, this change is across all particle sizes, whereas LECA retains the same percentage of particles over 5 mm in size. The increase in fines is clearly demonstrated in the median particle diameter (d_{50}) values of both substrates and in the percentage of particles finer than 0.063 mm. The dry density of the BBS substrate falls significantly between virgin and aged samples, whereas LECA samples exhibit a negligible change in dry density with age. Whilst both substrates exhibit increased MWHC with age, only the LECA substrate exhibits a statistically significant difference between the virgin and aged values of MWHC, increasing by approximately 7%.

3.2. XMT visual observations

Fig. 3 shows the physical differences between the compositions of the two substrate mixes, with LECA having a less dense particle matrix compared to BBS. Closer examination of the 2D slices shows the aged cores have more fine particles compared with their virgin counterparts. These slices also demonstrate the heterogeneous nature of the substrates, with clear differences in particle sizes and spacing between replicate cores of the same substrate and age.

3.3. XMT-derived substrate properties

Table 3 lists all XMT-derived parameters for the two substrate types and ages. Similarly, Fig. 4 presents the XMT-derived data for porosity, tortuosity (T^2) and saturated hydraulic conductivity (K_{sat}). Total porosity is separated into effective porosity (ϕ_E) and ineffective porosity (ϕ_I).

3.3.1. Porosity

Total porosity is elevated in LECA samples compared with the BBS samples (Fig. 4), due to a significantly higher amount of ineffective pore space. This is not unexpected due to the nature of the expanded clay mineral component of LECA. Mean values of porosity (Table 3) show a decline in both types of porosity in LECA substrates when comparing the virgin with aged samples, although these differences are not statistically significant. Total porosity of the virgin BBS samples is more consistent than within any other sample group. Across all BBS samples ineffective porosity is always negligible.

3.3.2. Particle size distribution

The XMT-derived particle size distributions for both substrate types indicate a shift towards a matrix with more fine particles with age (Fig. 5). The median particle diameter (d_{50}) decreased from 2.17 mm to 0.79 mm for BBS samples; this represents an 80% reduction. For LECA the median particle diameter fell from 2.53 mm to 0.42 mm, a reduction of 83%. The heterogeneity amongst the samples of the same substrate type and age is evident in the high values of standard deviation. The virgin BBS samples are much more alike than any other set of replicate age sample. This is consistent with the narrow range of porosity values identified for the virgin BBS substrate.

3.3.3. Pore size distribution

The pore size distributions also became finer with age (Fig. 5). This shift in pore sizes is more subtle than that seen for particle sizes. The median pore diameter of BBS samples fell by 58% from 1.01 mm to 0.42 mm. LECA samples saw a smaller reduction in median pore diameter, falling from 1.58 mm to 1.07 mm, a reduction of 32%. More heterogeneity can be seen in the pore size distributions for BBS than LECA, this is contrary to many of the other determinations of BBS properties. This observation is due to the increased complexity of the BBS matrix – with its angular particle shapes and smaller pores – compared to the more uniform LECA matrix.

3.3.4. Tortuosity

LECA substrates, of both ages, have a lower tortuosity compared to BBS (Fig. 4). This observation is consistent with the prior identification of saturated hydraulic conductivity (>30 mm/min vs. 1–35 mm/min for LECA and BBS respectively, Stovin et al., 2015a) and the less complex matrix of the LECA substrate. The tortuosity of BBS samples fell by 13% with age, whereas for LECA samples the reduction in tortuosity was greater, at 23%. Significant variation in the tortuosity values exists. However, due to the large number of values (N = 1000 per sample), Kruskal-Wallis tests indicated a significant statistical difference between the virgin and aged samples of both substrates.

3.3.5. Saturated hydraulic conductivity

Flow field visualisations from the LBM simulations show the formation of flow paths through the substrate mixes (Fig. 6). These visualisations are typical of the flow conditions seen throughout the substrate samples. However, the 2D images only represent a fraction of the samples, and features of interest have been highlighted to show the type of output generated by LBM simulations. The BBS examples show a single large flow path for the virgin sample compared to many smaller flow paths for the aged sample. The LECA examples both exhibit a flow path on the left edge of the image, the size and peak flow of the flow path in $LECA_A$ is narrower and slower compared to that of $LECA_V$.

Overall, aged samples have a lower saturated hydraulic conductivity (K_{sat}) than their virgin counterparts (Fig. 4). Although this difference is not statistically significant, a reduction in K_{sat} is to be expected given the reduction in porosity for aged samples seen in the XMT image analysis. With fewer pore spaces there are fewer flow paths, thereby restricting flow through the substrates. The relationship between BBS and LECA results is the same as that seen in Berretta et al. (2014) and Stovin et al. (2015a), whereby LECA has

Table 2
Physically determined properties of the BBS and LECA substrates (Mean values ± Standard Deviation).

Property	Unit	BBS		LECA	
		Virgin	Aged	Virgin	Aged
Particle Size <0.063 mm	%	0.38 ± 0.34*	1.41 ± 0.13*	0.66 ± 0.21*	1.57 ± 0.28*
Median Particle Diameter, d_{50}	mm	4.05 ± 0.40*	2.67 ± 0.16*	5.07 ± 0.40	5.01 ± 0.49
Dry Density	g/cm^3	0.94 ± 0.00*	0.75 ± 0.01*	0.66 ± 0.03	0. 65 ± 0.02
Density at Field Capacity	g/cm^3	1.21 ± 0.05*	1.08 ± 0.04*	0.87 ± 0.10	0. 93 ± 0.03
Max. water holding capacity, MWHC	% v/v	27.4 ± 5.08	33.3 ± 2.76	21.2 ± 6.89*	28.5 ± 1.05*

* Indicates significant statistical difference between the aged and virgin samples within each substrate type (Kruskal Wallis test, $P < 0.05$).

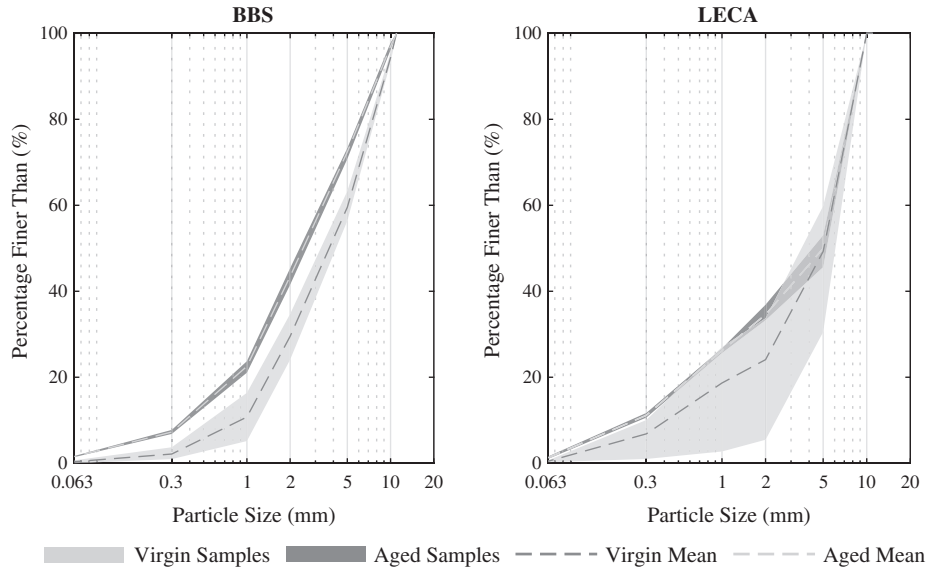

Fig. 2. Physically derived particle size distributions for the 12 substrate cores. Percentage by mass.

a higher K_{sat} than BBS. The virgin LECA samples have a very high standard deviation compared with all other samples. This is caused by sample $LECA_V1$ – which has been found to be consistently different across many properties – having a much higher K_{sat} than the other two virgin LECA samples. Excluding $LECA_V1$ from the analysis reveals a relationship much like that seen for BBS, with the aged substrate showing a reduction in mean K_{sat} of 27.8%.

3.4. Green roof hydrological modelling

3.4.1. Retention performance

The BBS and LECA substrates exhibited increased mean MWHC values in aged samples, +6 and +7% respectively (Table 2). A 7% increase in MWHC will lead to a 1.4 mm increase in S_{max} for an initial value of 20 mm, assuming PWP is constant with age. Fig. 7 shows the impact of this increase in S_{max}. Retention increases with increased ADWP due to the cumulative effects of ET. At a 28 day ADWP the difference in retention performance between virgin and aged substrates reaches its greatest extent of 4.7 percentage points for summer and 4.3 percentage points for spring. At low ADWPs (<4 days) the difference in retention performance between the virgin and aged substrates is just 2.5 percentage points in summer and 2.3 percentage points in spring. Fig. 7 also demonstrates the influence of climate on retention performance, where summer conditions – with greater PET – result in significantly enhanced retention performance compared to spring. For a 7-day spring ADWP the difference in aged retention performance resulting from climatic factors is 23.3 percentage points. This is 10 times greater than the difference resulting from ageing processes (2.3 percentage points).

The long-term simulation of the 30-year time-series for Sheffield, UK, found overall volumetric retention would increase by 1.4 percentage points for the aged substrate over the 30-year period. More importantly, the median retention during significant events (i.e. those with a return period of greater than one year) would increase by 2.3 percentage points.

3.4.2. Detention performance

The determined van Genuchten parameters of the BBS substrate allow an exploration of the relationship between hydraulic conductivity (K) and moisture content (θ). The $K(\theta)$ relationships for the two values of K_{sat} are presented in Fig. 8. At the onset of a rainfall event, moisture levels within the green roof substrate will be between the permanent wilting point (θ_{PWP}) and field capacity (θ_{FC}). Within this operational range, the differences between virgin and aged hydraulic conductivity are negligible. As the moisture content approaches saturation, the differences in hydraulic conductivity increase. However, even at typically observed maximum moisture contents (θ_{maxO}) (Berretta et al., 2014), the difference in hydraulic conductivity is still small compared to the difference in K_{sat} (0.14 vs. 16 mm/min).

In response to the design rainfall event, the virgin and aged saturated hydraulic conductivity values both result in significant reductions in the peak runoff rate (Fig. 9). The virgin BBS (K_{sat} = 38.9 mm/min) and aged BBS (K_{sat} = 22.9 mm/min) result in 70 and 80% peak attenuation respectively. However, the rainfall intensities of the design rainfall event are high in comparison to routine rainfall events.

When exploring the runoff detention response of the two differently aged systems to monitored rainfall patterns, the observable differences between them become much smaller (Fig. 9). For the virgin green roof system, peak attenuation of 28% is achieved, whilst the aged roof exhibits 31% peak attenuation. Again, the lower values of K_{sat} in the aged roof result in greater detention performance. However, in response to this monitored rainfall event the improvement between the virgin and aged systems is just 11% compared to a 14% increase for the design storm.

4. Discussion

4.1. Differences in virgin and aged substrate properties

For both the physical and XMT-based methods of investigation, particle sizes decreased with age. XMT-derived particle size distributions show greater reductions in median particle size for LECA than BBS. This is thought to demonstrate the fragility of the highly porous expanded clay aggregate within the LECA substrate, which is more prone to the destructive effects of weathering and root growth than the dense crushed brick of BBS. The observation of more fine particles in aged substrates is contrary to that reported by Bouzouidja et al. (2016), where the mass of particles with a diameter smaller than 2 mm in a pozzolana-based substrate fell

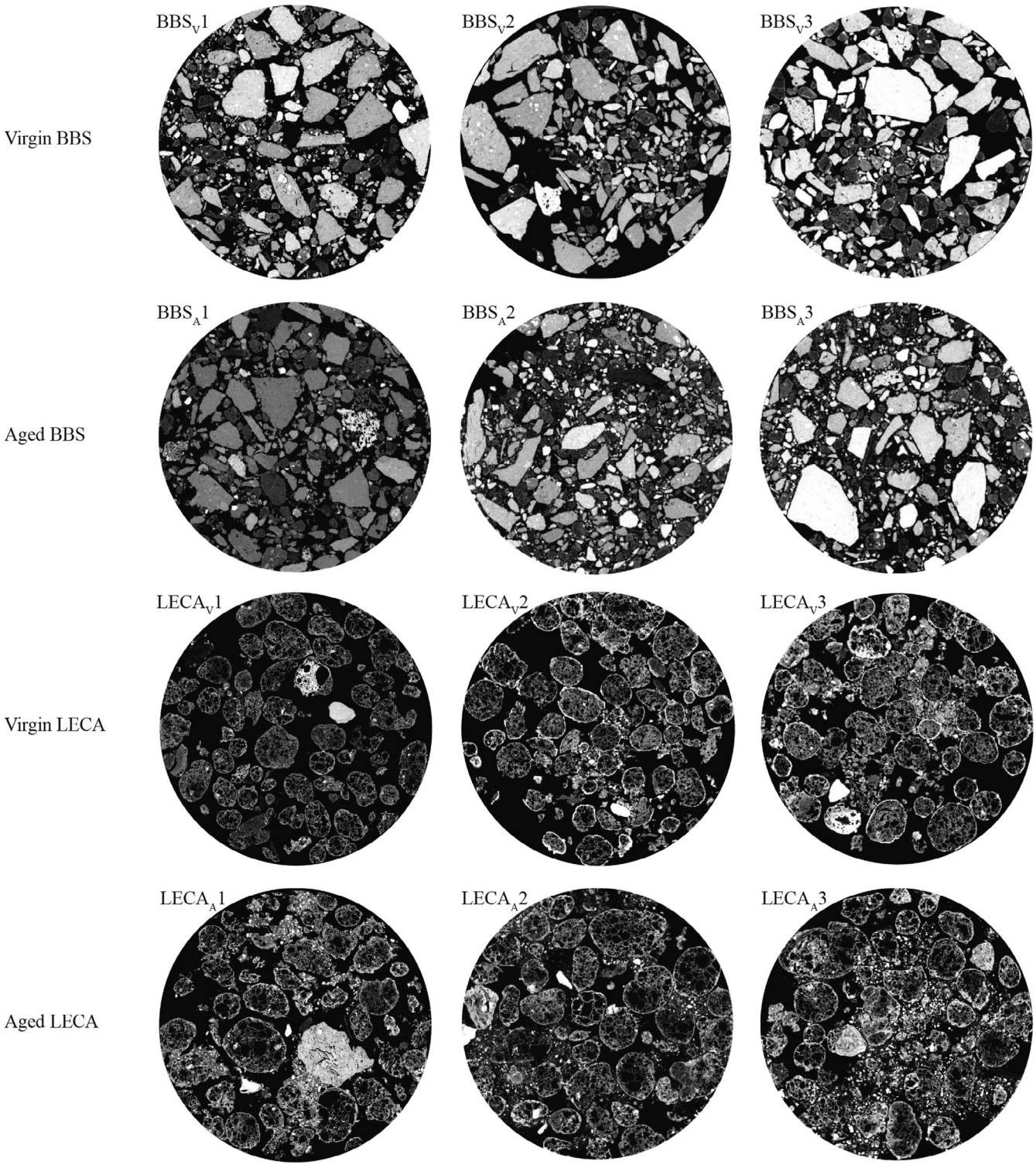

Fig. 3. Examples of raw XMT output for both the BBS and LECA substrates. 2D horizontal slices, all samples are 46 mm in diameter.

by up to 6% over a four-year period. This disparity, and the differences between BBS and LECA, highlight the variability in the impacts of ageing on differing substrate compositions.

Pore size reductions were inferred from the physically-derived MWHC values. As moisture is only held against gravity inside pores with a diameter smaller than 50 μm (Rowell, 1994), if the MWHC has increased then the total volume of pores with a diameter of <50 μm has also increased. As both virgin and aged samples are of the same total volume, then pores below 50 μm are more abundant in aged cores than their virgin counterparts, indicating a shift to smaller pore sizes. This is particularly evident in the LECA substrate, where sample density changes negligibly with age, but MWHC increases by 7%. Increases in MWHC were also seen by Getter et al. (2007) for a 60 mm depth of substrate. These increases in MWHC were attributed to increases in micropore (<50 μm) volumes. The XMT analysis similarly showed a reduction in pore sizes

Table 3
XMT-derived properties of the BBS and LECA substrates (Mean values ± Standard Deviation).

Property	Unit	BBS		LECA	
		Virgin	Aged	Virgin	Aged
Ineffective Porosity, ϕ_I	%	0.17 ± 0.01	0.22 ± 0.07	6.56 ± 3.14	6.36 ± 0.98
Effective Porosity, ϕ_E	%	35.6 ± 0.38	33.1 ± 6.44	39.9 ± 5.51	35.5 ± 8.16
Total Porosity, ϕ_T	%	35.8 ± 0.38	33.3 ± 6.37	46.5 ± 8.55	41.8 ± 7.30
Particle Size <0.063 mm	%	1.68 ± 0.84*	3.91 ± 0.37*	2.70 ± 2.44	5.54 ± 0.47
Median Particle Diameter, d_{50}	mm	2.17 ± 0.27*	0.79 ± 0.73*	2.53 ± 0.43*	0.42 ± 0.33*
Median Pore Diameter, d_{50}	mm	1.01 ± 0.39*	0.42 ± 0.11*	1.58 ± 0.23*	1.07 ± 0.21*
Tortuosity, T^2	–	6.93 ± 1.13*	5.99 ± 1.62*	6.54 ± 1.50*	5.05 ± 2.40*
Saturated Hydraulic Conductivity, K_{sat}	mm/min	38.7 ± 18.5	22.9 ± 5.60	179 ± 205	44.3 ± 31.8

* Indicates significant statistical difference between the aged and virgin samples within each substrate type (Kruskal Wallis test, $P < 0.05$).

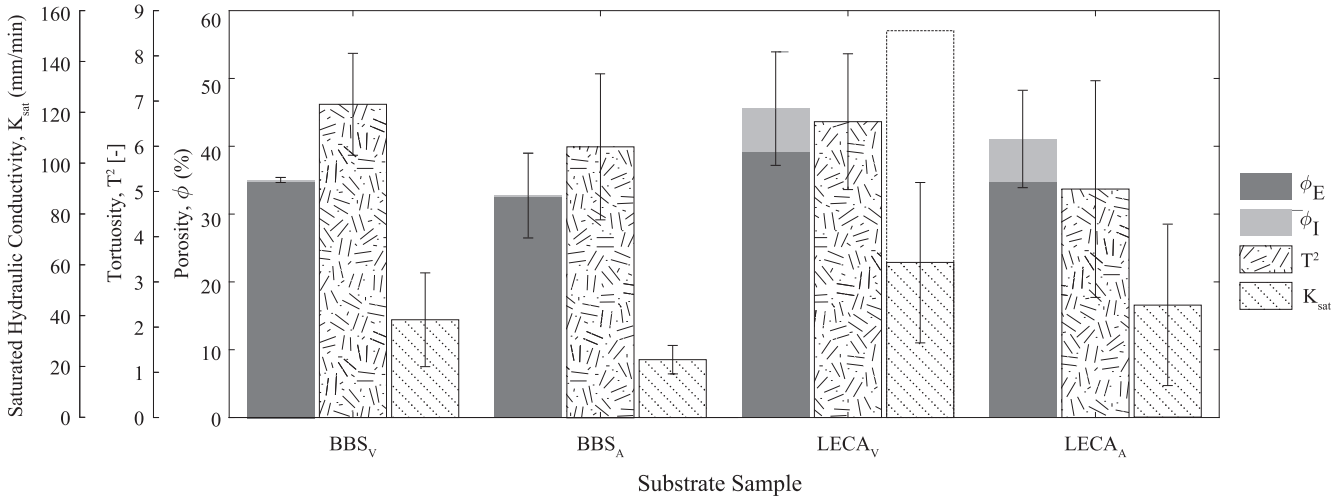

Fig. 4. XMT-derived physical property data. Dashed bar indicates mean Ksat for LECAV including result of LECAV1.

with increased substrate age. However, resolution limitations prevent accurate observation of changes in <50 μm diameter pore volumes. The increase in smaller pores is a result of root presence and the increased number of smaller particles within aged substrate matrices.

Pore size reductions are also indicative of substrate consolidation (Menon et al., 2015). Smaller pore networks reduce the cross sectional area for fluid flow and so have the effect of reducing hydraulic conductivity. The effect of this reduction in cross sectional area for fluid flow may be somewhat mitigated in this instance by the reductions in tortuosity for aged samples. Such reductions to tortuosity indicate a reduction in flow path lengths through the substrate, which would increase saturated hydraulic conductivity if it occurred in isolation (Schanz, 2007). However, results from the LBM simulations indicate that even with reductions in tortuosity, K_{sat} is lower for aged samples. In this case, it appears that pore size reductions are a more dominant component of hydraulic conductivity than tortuosity, as has previously been identified in soils by Vervoort and Cattle (2003).

Whilst differences are evident between the virgin and aged cores, care needs to be exercised in solely attributing these changes to age. The same manufacturer's substrate specification was used for both the aged and virgin cores. However, the samples were taken from different batches. Additionally, the aged samples were clearly not the original samples that had aged, but a different set of samples. Apparent differences in substrate properties could be attributable to substrate heterogeneity, given the relatively high standard deviations observed in most properties. Future studies of this type will need to take account of this, and it is recommended that the same sample be repeatedly examined throughout time as it ages. Such an experimental approach is only practical using non-destructive analysis techniques such as XMT.

4.2. Comparison of physically-derived and XMT-derived substrate properties

Two of the key physical properties that determine hydrological performance – porosity and saturated hydraulic conductivity – have been evaluated using both physical tests and XMT image analysis (Table 1). This allows for a comparison of the resultant property values and an evaluation of the usefulness of XMT. Whilst particle size distributions were also determined physically and via XMT-based methods, the two cannot be compared directly. The physically-derived particle size distribution is presented as a percentage by mass, whereas the XMT-derived particle size distribution is presented as a percentage by number.

The XMT-derived porosity values for both substrates are lower than the physically-derived values (Fig. 10). The greatest disparity is for aged LECA samples, where XMT-derived porosity (ϕ_{XMT}) is 25% lower than the observed porosity (ϕ_{Phys}). This discrepancy is caused by the XMT images having a resolution of 30 μm. Any features smaller than this cannot be resolved and so are not represented in characterised property values. Values of MWHC determined from physical tests give some indication of the porosity for pores smaller than 50 μm, as this approximate pore size corresponds to field capacity conditions. Addition of the MWHC values to XMT derived porosities typically gives total porosity values in excess of those determined physically (Fig. 10). This is to be expected as there is some overlap between the 30 μm XMT limit and the 50 μm criteria for field capacity. Given the above, ϕ_{XMT}

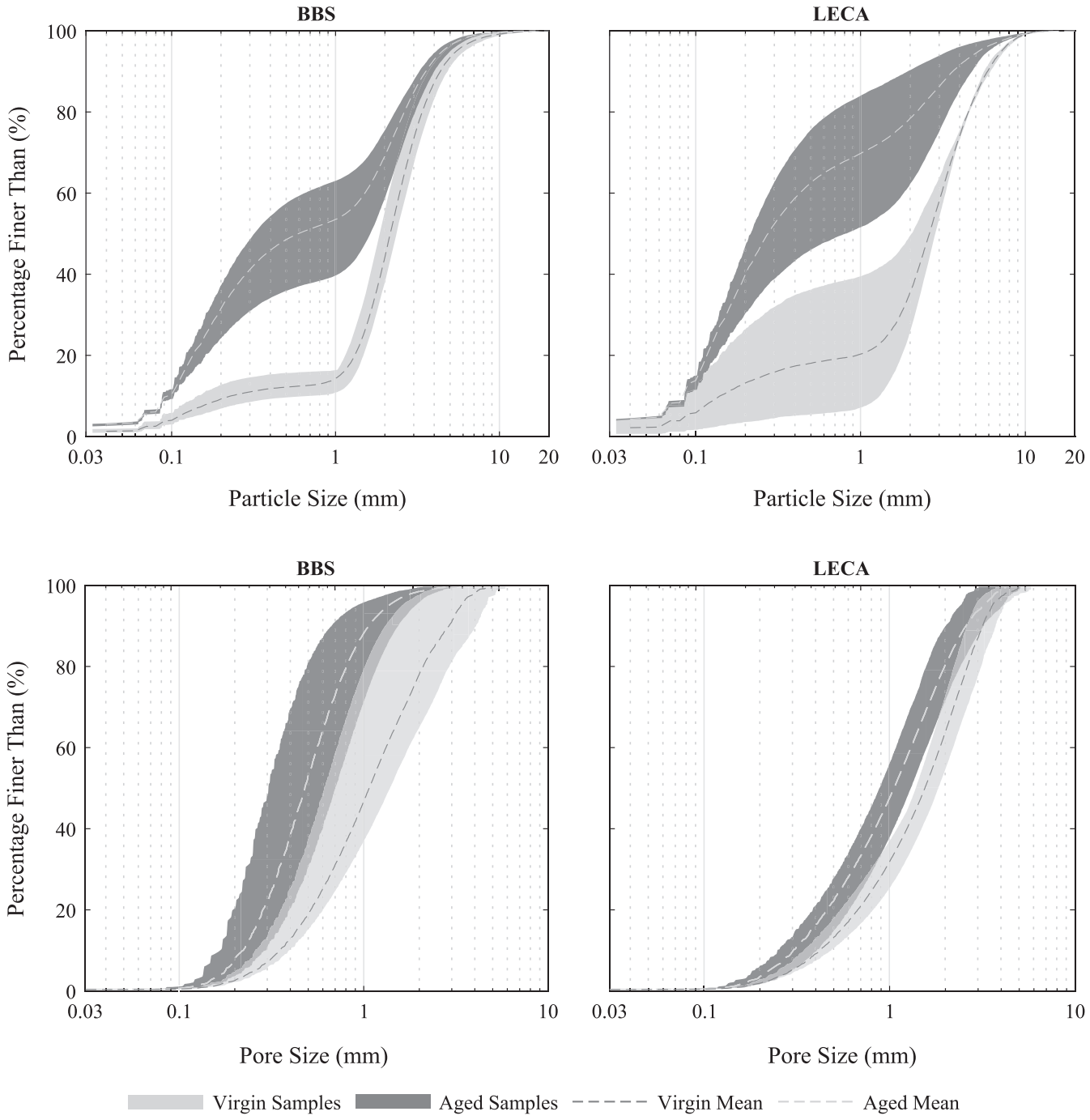

Fig. 5. XMT-derived particle and pore size distributions.

appears to be a reasonable characterisation of sample porosity for pore sizes greater than 30 μm.

K_{sat} compares favourably between the physically-derived values of Stovin et al. (2015a) (BBS_{Phys} and $LECA_{Phys}$) and XMT-derived values (BBS_V, BBS_A, $LECA_V$, $LECA_A$), with LECA substrates consistently showing elevated levels of saturated hydraulic conductivity over BBS (Fig. 10). XMT-derived values are slightly elevated (when not including the $LECA_V1$ sample) over physically-derived values, this is expected as a result of the resolution limit on the XMT data. Only those flow paths with a diameter of >30 μm are modelled, with narrower flow paths – which may support slower velocities – being excluded. As the XMT-derived values are determined from the superficial velocity of the fluid flow (mean velocity) the omission of zones with slower flow skews the result toward a higher value of K_{sat}.

The disparities between physical and XMT-based determinations of porosity and saturated hydraulic conductivity can be largely attributed to the resolution of the XMT scan, and highlight the importance of acquiring images with sufficient resolution to resolve the features of interest. With current equipment, high image resolutions (<5 μm) require very small sample sizes (<5 mm in diameter). Soil science studies advocate the use of the smallest sample possible to maximise image resolution, with a core diameter of 50 mm being optimal (Rab et al., 2014). In this study, the heterogeneity of the substrate prevented the use of smaller diameter samples. Previous XMT studies of heterogeneous

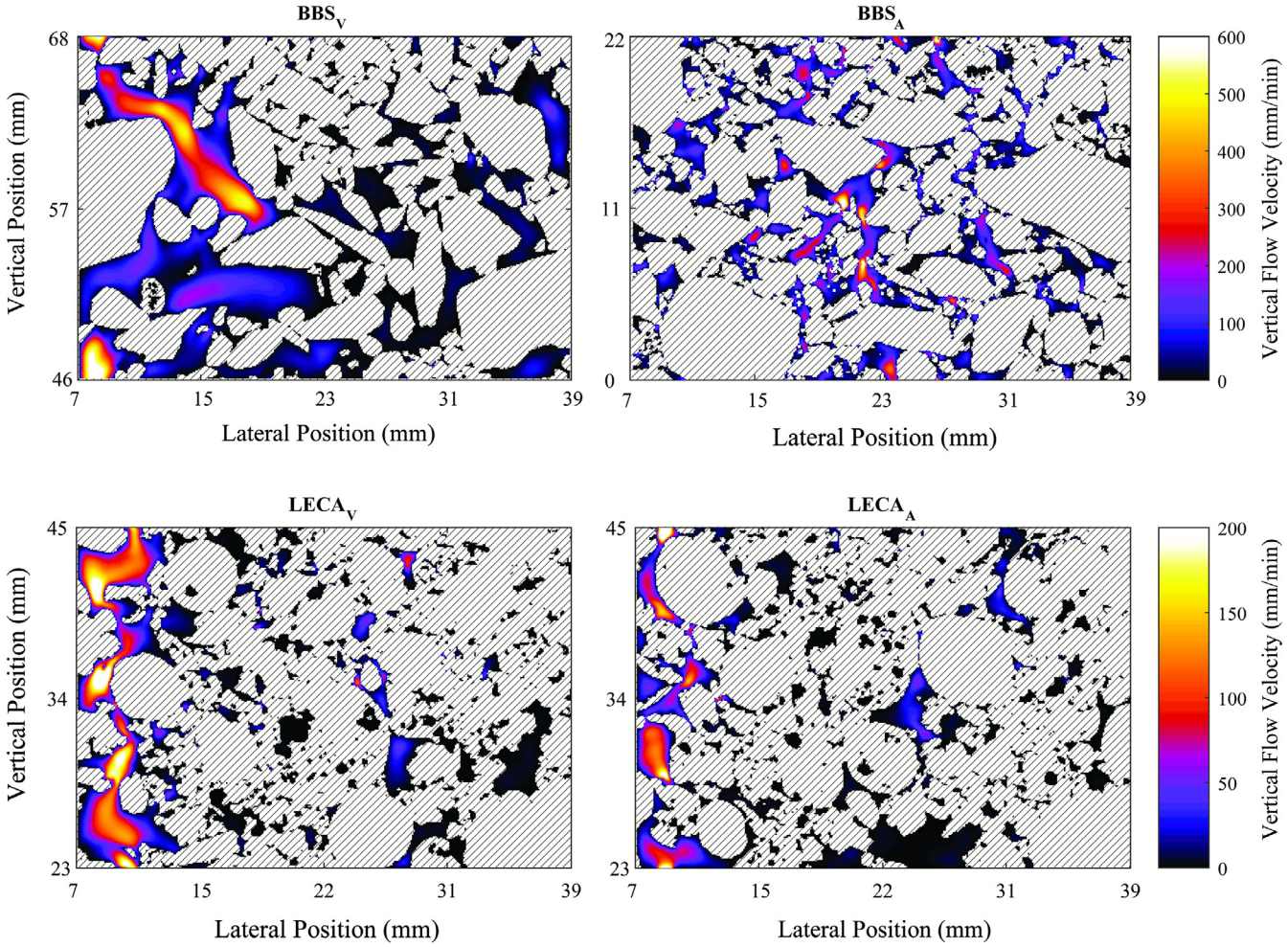

Fig. 6. LBM flow field visualisations. Hatched areas indicate solid particle spaces. Top: brick-based substrate. Bottom: LECA substrate. *Note:* BBS and LECA use different velocity scales.

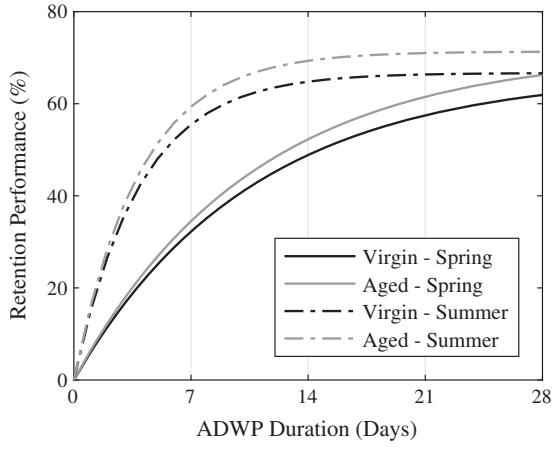

Fig. 7. Comparison of the potential retention performance for a virgin and aged green roof under different climatic conditions.

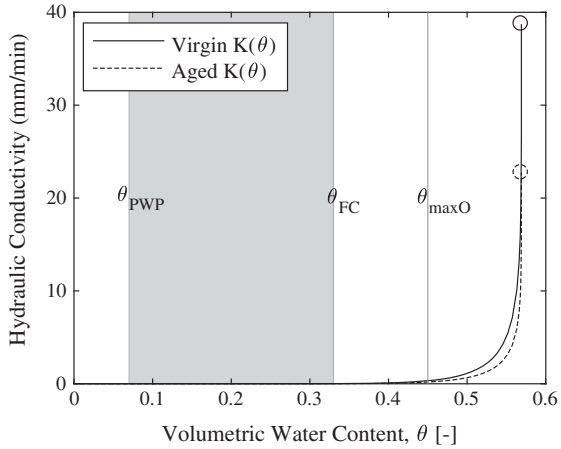

Fig. 8. K(θ) relationship for BBS mean virgin and aged Ks. Circular points indicate Ks. Shaded region represents typical operational moisture content at storm onset.

media (glass beads and sands) identified that the effects of heterogeneity are minimised for samples where the core diameter is 2–20 times the largest particle diameter (Costanza-Robinson et al., 2011). For the 46 mm diameter cores of this study a core diameter to maximum particle diameter ratio of 2.87 (median value) was achieved, i.e. within the target 2–20 range. It may be argued that a successful compromise has been achieved in maximising XMT image resolution whilst mitigating against excessive heterogeneity influences.

Whilst some disparities between physically and XMT-derived properties were noted, consistent general trends in the relative differences between the quantified properties of the two substrates over time were observed. The XMT technique allowed for the

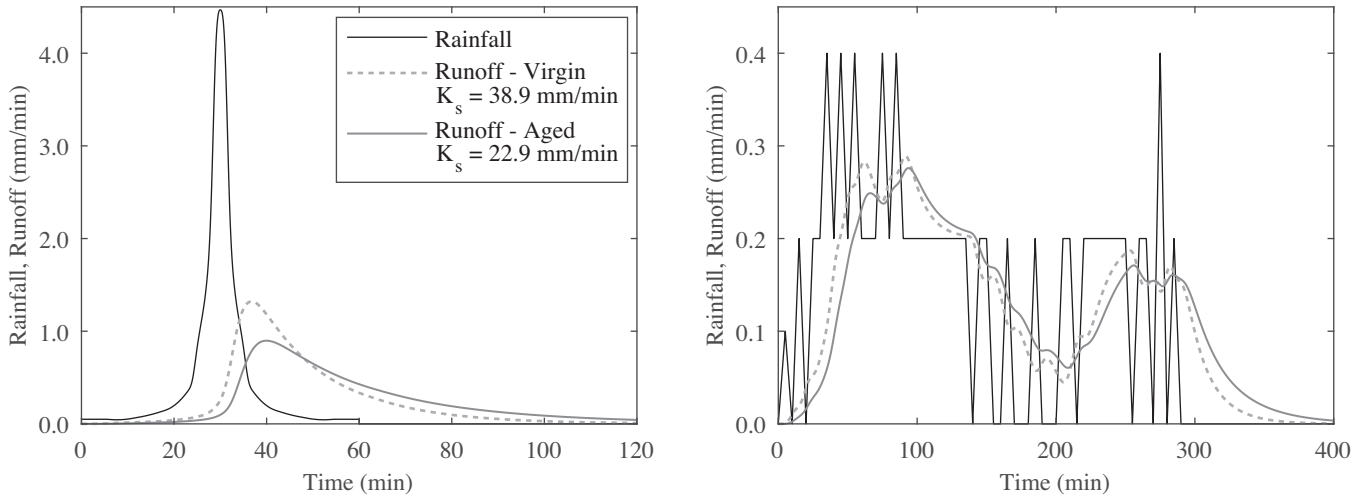

Fig. 9. Detention only runoff response for two values of Ks. Left: Response to a 1 h 1-in-30-year design storm for Sheffield, UK, P = 30.28 mm. Right: Response to a monitored rainfall event in Sheffield, UK, P = 9.5 mm.

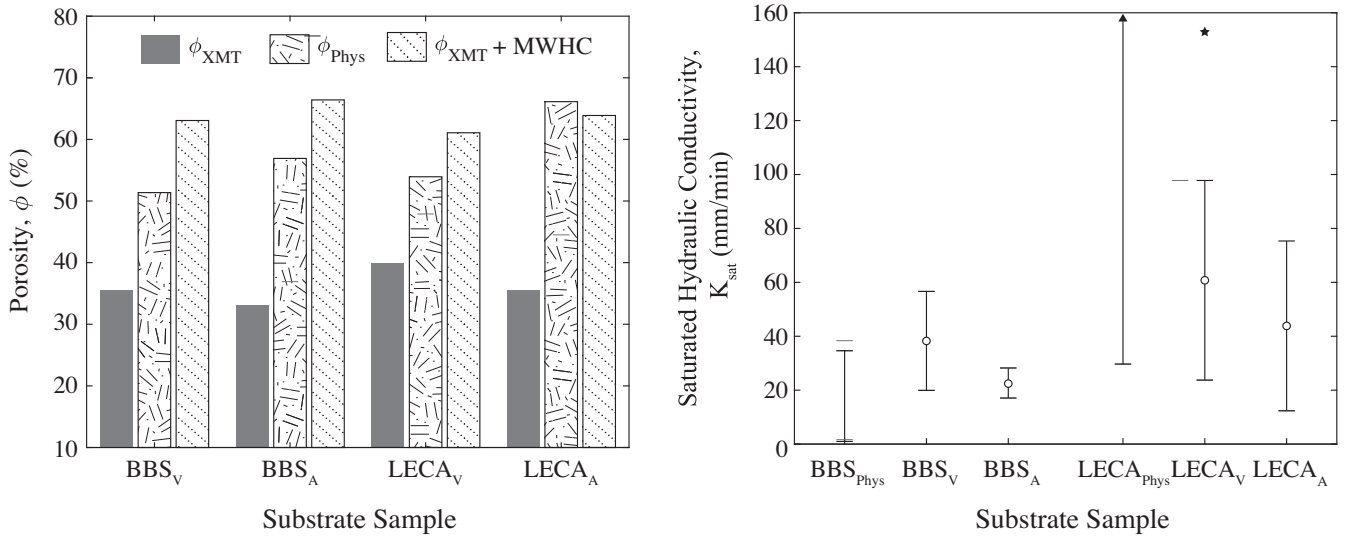

Fig. 10. Comparison of physically-derived and XMT-derived property values. Left: Porosity, mean values for each sample group. Including XMT-derived porosity + physically observed MWHC. Right: Saturated hydraulic conductivity, results of this study plotted as mean and standard deviation, physically-derived Stovin et al. (2015a,b) values plotted as a range. Pentagram indicates mean of LECAV including result for LECAV1.

non-destructive characterisation of key substrate properties. It is this non-destructive nature that is the greatest benefit of using XMT for assessing the evolution of green roof substrate properties over time. The repeated imaging of the same substrate sample will allow for the determination of key property evolutions associated with ageing whilst removing the uncertainty of substrate heterogeneity.

4.3. Implications of substrate property changes on hydrological performance

4.3.1. Retention performance

The improvements seen in retention performance due to increasing substrate age are small (<5%, at their greatest extent). Long-term simulation of retention performance yields improvements that are a third the size of those seen for the design storm after a prolonged (28-day) ADWP. This is not unexpected, as natural ADWPs are typically much lower than 28 days.

To determine an aged and virgin value of S_{max} for the retention modelling it was assumed that PWP was constant over time. Such an assumption may not be correct. The XMT-derived pore size distributions for both substrates suggest a reduction in pore diameters. Any increase in the total volume of pores below 0.2 μm will lead to increases in the value of PWP. Bouzouidja et al. (2016) observed moderate increases in PWP from 7 to 12% over a 4-year period in a pozzolana-based green roof substrate. This increase in PWP was directly attributed to the number of pores <0.2 μm in diameter and contributed to PAW reducing from an initial 11%, to just 2% within 4 years. The virgin BBS samples of this study have a PAW of >20% using the PWP value of comparable brick-based substrates from Berretta et al. (2014). Given that aged substrates have a MWHC of 33% (compared to 27% for virgin substrates), PWP would have to double to result in any overall reduction in PAW. To see similar declines in PAW as Bouzouidja et al. (2016), the PWP of BBS would need to of have quadrupled in 5 years. It is therefore possible that actual retention performance improvements may be smaller than those modelled here. However, from current observations, it is unlikely that the retention performance of a crushed-brick-based substrate will decline within a 5-year period due to changes in substrate properties.

4.3.2. Detention performance

Reductions in saturated hydraulic conductivity for the aged substrate samples are associated with an improvement in detention performance. Such an observation was expected due to the increase in the physical travel times of flow through the substrate. These observations are in line with the laboratory study findings of Yio et al. (2013) and those of the Stovin et al. (2015a) monitoring study. As there are no statistically significant differences between the virgin and aged values of K_{sat} for the BBS substrate, the resulting runoff profiles also have no statistically significant differences.

The input data for the modelling approach employed within this study is a simplification of the very complex relationships between hydraulic conductivity, tortuosity and pore size distributions. A single set of van Genuchten parameters was used to describe both the virgin and aged BBS substrate. Given the absence of water release data for the samples of this study, the results of comparable brick-based substrates were used from Berretta et al. (2014). Whilst there is little deviation between the water release curves of the two substrates presented in Berretta et al. (2014) and other unpublished works, the subtleties of differences in tortuosity and pore size distributions will have an impact on hydraulic conductivity, particularly for low moisture contents. Ongoing work is exploring the possibility of determining a $K(\theta)$ relationship from the XMT and LBM approaches, this will provide an alternative to traditional water release relationship determinations. Such an approach will also allow for greater investigation of the relationships between pore sizes, tortuosity and K_{sat}.

4.3.3. Practical implications

The small improvements to both retention and detention expected over time are unlikely to be detected in practical field monitoring programmes. Any variation resulting from substrate property changes is small compared to climatic and seasonal variations. This, alongside the lack of statistical differences between the virgin and aged substrates, supports the findings of Mentens et al. (2006), where no statistical significance was found between green roof hydrological performance and system age. The fact that there are no indications that hydrological performance will have declined in a 5-year period of normal operation may be of most importance to urban planners and stormwater engineers.

5. Conclusions

This study used non-invasive XMT techniques alongside traditional physical testing to evaluate the differences in green roof substrate arising from ageing processes. Significant differences were observed within the physical structure of the crushed brick substrate when comparing virgin and aged samples. However, these structural differences did not lead to any statistically significant differences in key hydrological characteristics (MWHC and K_{sat}). For the LECA substrate, there were fewer structural differences between the virgin and aged substrate samples, with the largest differences being for the percentage of fine particles (<0.063 mm) and median pore sizes. The LECA substrate exhibited a significant increase in MWHC of 7% with age. This increased MWHC is attributed to the changes within the substrate matrix, with a shift toward smaller pore sizes.

Observed increases in MWHC facilitate greater retention performance, but, the changes observed in retention performance with age are an order of magnitude smaller than retention performance differences due to seasonal variations in ET. It is therefore unlikely that any improvements in MWHC would be detected in full-scale monitoring studies. Although there were no statistically significant differences in K_{sat} values with age for either substrate, the wide range of K_{sat} values led to visibly different runoff responses. A reduction in K_{sat} of ~40% resulted in up to a 14% increase in peak attenuation for a design storm, indicating improved detention performance.

The complex relationship between hydraulic conductivity, tortuosity and pore sizes remains a significant barrier to the better understanding of the hydrological performance of green roofs and other green infrastructure systems. However, a combination of the non-invasive XMT and LBM approaches could provide a promising new method for the determination of a $K(\theta)$ relationship.

X-ray microtomography has proven to be a powerful tool for the visualisation of the internal structure of green roof substrates. In turn, this has allowed for the non-destructive determination of several physical properties that are key to understanding hydrological performance. Whilst some disparities between physically and XMT-derived properties were noted, consistent general trends in the relative differences between the quantified properties of the two substrates over time were observed. Many of the disparities between physically and XMT-derived properties are attributable to the XMT image resolution. It is therefore important that guidance presented in previous literature is followed regarding sample size, with sample core diameters exceeding double the largest particle diameter. Such steps help to mitigate heterogeneity effects, reduce required sample replication, maximise image resolution and therefore maximise XMT data quality.

Acknowledgements

This work was supported by the Pennine Water Group of the University of Sheffield in turn supported by the Engineering and Physical Sciences Research Council (EPSRC) [grant number EP/I029346/1]. Simon De-Ville is supported by an EPSRC DTA Award [grant number EP/L505055/1]. The authors would like to thank Prof. Sacha Mooney and Dr. Craig Sturrock from the Hounsfield Facility at the University of Nottingham for the use of their XMT facilities. The authors would also like to thank the reviewers for their time, effort, and comments in helping to improve this manuscript.

Appendix A. Supplementary data – Image processing protocol

Supplementary data associated with this article can be found, in the online version, at http://dx.doi.org/10.1016/j.jhydrol.2017.02.006.

References

Bayton, S., 2013. Hydraulic Performance of a Green Roof Substrate (MEng Dissertation). University of Sheffield, Sheffield, UK.

Berndtsson, J.C., 2010. Green roof performance towards management of runoff water quantity and quality: a review. Ecol. Eng. 36, 351–360. http://dx.doi.org/10.1016/j.ecoleng.2009.12.014.

Berretta, C., Poë, S., Stovin, V., 2014. Moisture content behaviour in extensive green roofs during dry periods: the influence of vegetation and substrate characteristics. J. Hydrol. 511, 374–386. http://dx.doi.org/10.1016/j.jhydrol.2014.01.036.

Bouzouidja, R., Rousseau, G., Galzin, V., Claverie, R., Lacroix, D., Séré, G., 2016. Green roof ageing or isolatic technosol's pedogenesis? J. Soils Sediments. http://dx.doi.org/10.1007/s11368-016-1513-3.

Carson, T.B., Marasco, D.E., Culligan, P.J., McGillis, W.R., 2013. Hydrological performance of extensive green roofs in New York city: observations and multi-year modeling of three full-scale systems. Environ. Res. Lett. 8, 024036. http://dx.doi.org/10.1088/1748-9326/8/2/024036.

Costanza-Robinson, M.S., Estabrook, B.D., Fouhey, D.F., 2011. Representative elementary volume estimation for porosity, moisture saturation, and air-water interfacial areas in unsaturated porous media: data quality implications. Water Resour. Res. 47. http://dx.doi.org/10.1029/2010wr009655. n/a–n/a.

Dexter, A.R., 1987. Compression of soil around roots. Plant Soil 97, 401–406. http://dx.doi.org/10.1007/bf02383230.

Emilsson, T., Rolf, K., 2005. Comparison of establishment methods for extensive green roofs in southern Sweden. Urban For. Urban Greening 3, 103–111. http://dx.doi.org/10.1016/j.ufug.2004.07.001.

Fassman-Beck, E., Voyde, E., Simcock, R., Hong, Y.S., 2013. 4 living roofs in 3 locations: does configuration affect runoff mitigation? J. Hydrol. 490, 11–20. http://dx.doi.org/10.1016/j.jhydrol.2013.03.004.

FEI, 2015. Aviso user's guide [WWW Document] URL http://www.vsg3d.com/sites/default/files/AvizoUsersGuide.pdf (accessed 6.12.15).

FLL, 2008. Guidelines for the Planning, Construction and Maintenance of Green Roofing. Forschungsgesellschaft Landschaftsentwicklung Landschaftsbau e.V, Bonn, Germany.

Getter, K.L., Rowe, B.D., Andresen, J.A., 2007. Quantifying the effect of slope on extensive green roof stormwater retention. Ecol. Eng. 31, 225–231. http://dx.doi.org/10.1016/j.ecoleng.2007.06.004.

Harper, G.E., Limmer, M.A., Showalter, E.W., Burken, J.G., 2015. Nine-month evaluation of runoff quality and quantity from an experiential green roof in Missouri, USA. Ecol. Eng. 78, 127–133. http://dx.doi.org/10.1016/j.ecoleng.2014.06.004.

Hilten, R.N., Lawrence, T.M., Tollner, E.W., 2008. Modeling stormwater runoff from green roofs with HYDRUS-1D. J. Hydrol. 358, 288–293. http://dx.doi.org/10.1016/j.jhydrol.2008.06.010.

Jarrett, A.R., Berghage, R.D., 2008. Annual and individual green roofs stormwater response models. The 6th Greening Rooftops for Sustainable Communities Conference. Baltimore, MD.

Kasmin, H., Stovin, V.R., Hathway, E.A., 2010. Towards a generic rainfall-runoff model for green roofs. Water Sci. Technol. 62. http://dx.doi.org/10.2166/wst.2010.352.

Lado, M., Paz, A., Ben-Hur, M., 2004. Organic matter and aggregate size interactions in infiltration, seal formation, and soil loss. Soil Sci. Soc. Am. J. 68, 935. http://dx.doi.org/10.2136/sssaj2004.9350.

Li, Y., Babcock, R.W., 2014. Green roof hydrologic performance and modeling: a review. Water Sci. Technol. 69. http://dx.doi.org/10.2166/wst.2013.770.

Locatelli, L., Mark, O., Mikkelsen, P.S., Arnbjerg-Nielsen, K., Jensen, M.B., Binning, P.J., 2014. Modelling of green roof hydrological performance for urban drainage applications. J. Hydrol. 519, 3237–3248. http://dx.doi.org/10.1016/j.jhydrol.2014.10.030.

Maire, E., Withers, J., 2014. Quantitative X-ray tomography. Int. Mater. Rev. http://dx.doi.org/10.1179/1743280413Y.0000000023.

Materechera, S.A., Dexter, A.R., Alston, A.M., 1992. Formation of aggregates by plant roots in homogenised soils. Plant Soil 142, 69–79. http://dx.doi.org/10.1007/BF00010176.

Menon, M., Jia, X., Lair, G.J., Faraj, P.H., Blaud, A., 2015. Analysing the impact of compaction of soil aggregates using X-ray microtomography and water flow simulations. Soil Tillage Res. 150, 147–157. http://dx.doi.org/10.1016/j.still.2015.02.004.

Menon, M., Yuan, Q., Jia, X., Dougill, A.J., Hoon, S.R., Thomas, A.D., Williams, R.A., 2011. Assessment of physical and hydrological properties of biological soil crusts using X-ray microtomography and modeling. J. Hydrol. 397, 47–54. http://dx.doi.org/10.1016/j.jhydrol.2010.11.021.

Mentens, J., Raes, D., Hermy, M., 2006. Green roofs as a tool for solving the rainwater runoff problem in the urbanized 21st century? Landscape Urban Plann. 77, 217–226. http://dx.doi.org/10.1016/j.landurbplan.2005.02.010.

Nawaz, R., McDonald, A., Postoyko, S., 2015. Hydrological performance of a full-scale extensive green roof located in a temperate climate. Ecol. Eng. 82, 66–80. http://dx.doi.org/10.1016/j.ecoleng.2014.11.061.

Palla, A., Gnecco, I., Lanza, L.G., 2011. Compared performance of a conceptual and a mechanistic hydrologic models of a green roof. Hydrol. Process. 26, 73–84. http://dx.doi.org/10.1002/hyp.8112.

Poë, S., Stovin, V., Berretta, C., 2015. Parameters influencing the regeneration of a green roof's retention capacity via evapotranspiration. J. Hydrol. 523, 356–367. http://dx.doi.org/10.1016/j.jhydrol.2015.02.002.

Rab, M.A., Haling, R.E., Aarons, S.R., Hannah, M., Young, I.M., Gibson, D., 2014. Evaluation of X-ray computed tomography for quantifying macroporosity of loamy pasture soils. Geoderma 213, 460–470. http://dx.doi.org/10.1016/j.geoderma.2013.08.037.

Rowell, D.L., 1994. Soil Science. Methods and Applications – David L. Rowell – Paperback. Addison Wesley Longman, Harlow, Essex, New York.

Schanz, T., 2007. Experimental Unsaturated Soil Mechanics. Springer-Verlag, Berlin and Heidelberg GmbH & Co. K, Berlin.

Schneider, C.A., Rasband, W.S., Eliceiri, K.W., 2012. NIH image to ImageJ: 25 years of image analysis. Nat. Methods 9, 671–675. http://dx.doi.org/10.1038/nmeth.2089.

Schwen, A., Bodner, G., Scholl, P., Buchan, G.D., Loiskandl, W., 2011. Temporal dynamics of soil hydraulic properties and the water-conducting porosity under different tillage. Soil Tillage Res. 113, 89–98. http://dx.doi.org/10.1016/j.still.2011.02.005.

Stovin, V., Poë, S., Berretta, C., 2013. A modelling study of long term green roof retention performance. J. Environ. Manage. 131, 206–215. http://dx.doi.org/10.1016/j.jenvman.2013.09.026.

Stovin, V., Poë, S., De-Ville, S., Berretta, C., 2015a. The influence of substrate and vegetation configuration on green roof hydrological performance. Ecol. Eng. 85, 159–172. http://dx.doi.org/10.1016/j.ecoleng.2015.09.076.

Stovin, V., Vesuviano, G., De-Ville, S., 2015b. Defining green roof detention performance. Urban Water J. 1–15. http://dx.doi.org/10.1080/1573062x.2015.1049279.

Stovin, V., Vesuviano, G., Kasmin, H., 2012. The hydrological performance of a green roof test bed under UK climatic conditions. J. Hydrol. 414–415, 148–161. http://dx.doi.org/10.1016/j.jhydrol.2011.10.022.

Taina, I.A., Heck, R.J., Elliot, T.R., 2008. Application of x-ray computed tomography to soil science: A literature review. Can. J. Soil Sci. 88, 1–19. http://dx.doi.org/10.4141/cjss06027.

Thuring, C.E., Dunnett, N., 2014. Vegetation composition of old extensive green roofs (from 1980s Germany). Ecol. Processes 3. http://dx.doi.org/10.1186/2192-1709-3-4.

van Genuchten, M.T., 1980. A closed-form equation for predicting the hydraulic conductivity of unsaturated soils. Soil Sci. Soc. Am. J. 44 (5), 892–898.

van Genuchten, M.T., Leij, F.J., Yates, S.R., 1991. The RETC Code for Quantifying the Hydraulic Functions of Unsaturated Soils, Version 1.0: EPA Report 600/2-91/065. U.S. Salinity Laboratory, USDA, ARS, Riverside, California.

Vervoort, R.W., Cattle, S.R., 2003. Linking hydraulic conductivity and tortuosity parameters to pore space geometry and pore-size distribution. J. Hydrol. 272, 36–49. http://dx.doi.org/10.1016/S0022-1694(02)00253-6.

Villarreal, E.L., Bengtsson, L., 2005. Response of a green-roof to individual rain events. Ecol. Eng. 25, 1–7. http://dx.doi.org/10.1016/j.ecoleng.2004.11.008.

Virahsawmy, H.K., Stewardson, M.J., Vietz, G., Fletcher, T.D., 2014. Factors that affect the hydraulic performance of raingardens: implications for design and maintenance. Water Sci. Technol. 69, 982. http://dx.doi.org/10.2166/wst.2013.809.

Wilson, E.M., 1990. Engineering Hydrology. Palgrave Macmillan, London, Angleterre.

Yio, M.H.N., Stovin, V., Werdin, J., Vesuviano, G., 2013. Experimental analysis of green roof substrate detention characteristics. Water Sci. Technol. 68. http://dx.doi.org/10.2166/wst.2013.381.

Young, I., Crawford, J., Rappoldt, C., 2001. New methods and models for characterising structural heterogeneity of soil. Soil Tillage Res. 61, 33–45. http://dx.doi.org/10.1016/s0167-1987(01)00188-x.